4392 *Chem. Mater.* **2010,** *22,* 4392–4399
DOI:10.1021/cm100770x

CHEMISTRY OF MATERIALS
Article

# Toward Optimization of Oligothiophene Antennas: New Ruthenium Sensitizers with Excellent Performance for Dye-Sensitized Solar Cells

Jen-Fu Yin,[‡] Jian-Ging Chen,[§] Zong-Zhan Lu,[†] Kuo-Chuan Ho,[§] Hong-Cheu Lin,*[,‡] and Kuang-Lieh Lu*[,†]

[†]*Institute of Chemistry, Academia Sinica, Taipei 115, Taiwan,* [‡]*Department of Materials Science and Engineering, National Chiao Tung University, Hsinchu 300, Taiwan, and* [§]*Department of Chemical Engineering, National Taiwan University, Taipei 106, Taiwan*

*Received March 16, 2010. Revised Manuscript Received June 9, 2010*

This paper reports on the design and synthesis of three new ruthenium sensitizers, as well as the optimization of their linear or dendritic light-harvesting oligothiophene antennas to achieve superior device performance. The three new ruthenium sensitizers, [Ru(dcbpy)(obtip)(NCS)$_2$] (**JF-5**, dcbpy = 4,4′-dicarboxylic acid-2,2′-bipyridine, obtip = 2-(5-octyl-(2,2′-bithiophen)-5′-yl)-1*H*-imidazo[4,5-*f*][1,10]-phenanthroline), [Ru(dcbpy)(ottip)(NCS)$_2$] (**JF-6**, ottip = 2-(5-octyl-2,2′,5′,2″-terthiophen)-5″-yl)-1*H*-imidazo[4,5-*f*][1,10]phenanthroline), and [Ru(dcbpy)(dottip)(NCS)$_2$] (**JF-7**, dottip = 2-(2,3-di-(5-octylthiophen-2-yl)thiophen-5-yl)-1*H*-imidazo[4,5-*f*][1,10]phenanthroline), were synthesized in a typical one-pot reaction. The ruthenium sensitizer **JF-5** incorporating a linear and planar 2,2′-bithiophene antenna showed the best DSCs performance (9.5%; compared to **N3**, 8.8%). The difference in the performance of these sensitizers demonstrates that elongating the linear and planar light-harvesting antenna result in an enhancement in MLCT intensity, but a reduction in the quantity of dye-loading. This finding not only permitted the power-conversion efficiency in ruthenium sensitizers containing oligothiophene antennas to be optimized, but also points to a promising direction for molecule engineering in DSCs.

## Introduction

With the likely increase in oil prices on the horizon, the development of alternative energy sources has become a subject of major research interest. The solar energy incident on the earth's surface, whose globally convertible power is estimated to be 120000 TW, constitutes an inexhaustible, plentiful, and clean energy source, which is sufficient to satisfy the world's needs.[1] Therefore, the practical and efficient use of solar energy has been a consistently significant topic in recent years. The dye-sensitized solar cells (DSCs) have great potential for replacing traditional silicon solar cells because of their high photon-to-current conversion efficiency, ease, and low cost of preparation.[2,3] The best power-conversion efficiency (up to 11%) was achieved by using ruthenium-based dyes in DSCs, such as **N3**- and **N719**-sensitized solar cells.[4,5] Attempts to design and synthsize new heteroleptic ruthenium sensitizers with higher device performances is ongoing.[6−15] There are two crucial factors that affect the performance of DSCs, the intensity of the metal-to-ligand charge transfer (MLCT) band[16,17] and the quantity of dye that can be loaded.[18,19] Several groups have modified ancillary ligands in ruthenium complexes by elongating[20−22] or bifurcating[23,24] conjugated light-harvesting

*To whom correspondence should be addressed. Fax: +886-2-27831237. E-mail: lu@chem.sinica.edu.tw.

(1) Basic Research Needs for Solar Energy Utilization, BES Workshop on Solar Energy Utilization, April 18−25, **2005**.
(2) O'Regan, B.; Grätzel, M. *Nature* **1991**, *353*, 737.
(3) Grätzel, M. *Nature* **2001**, *414*, 338.
(4) Nazeeruddin, M. K.; Key, A.; Rodicio, L.; Humphrey-Baker, R.; Müller, E.; Liska, P.; Vlachopoulos, N.; Grätzel, M. *J. Am. Chem. Soc.* **1993**, *115*, 6382.
(5) Nazeeruddin, M. K.; Zakeeruddin, S. M.; Humphry-Baker, R.; Jirousek, M.; Liska, P.; Vlachopoulos, N.; Shklover, V.; Fischer, C.-H.; Grätzel, M. *Inorg. Chem.* **1999**, *38*, 6298.
(6) Wang, P.; Klein, C.; Humphrey-Baker, R.; Zakeeruddin, S. M.; Grätzel, M. *J. Am. Chem. Soc.* **2005**, *127*, 808.
(7) Jiang, K.-J.; Masaki, N.; Xia, J.-b.; Noda, S.; Yanagida, S. *Chem. Commun.* **2006**, 2460.
(8) Chen, C. Y.; Wu, S. J.; Wu, C. G.; Chen, J. G.; Ho, K. C. *Angew. Chem., Int. Ed.* **2006**, *45*, 5822.
(9) Chen, C. Y.; Wu, S. J.; Li, J. Y.; Wu, C. G.; Chen, J. G.; Ho, K. C. *Adv. Mater.* **2007**, *19*, 3888.
(10) Matar, F.; Ghaddar, T. H.; Walley, K.; DosSantos, T.; Durrant, J. R.; O'Regan, B. *J. Mater. Chem.* **2008**, *18*, 4246.
(11) Gao, F.; Wang, Y.; Zhang, J.; Shi, D.; Wang, M.; Humphry-Baker, R.; Wang, P.; Zakeeruddin, S. M.; Grätzel, M. *Chem. Commun.* **2008**, 2635.
(12) Gao, F.; Wang, Y.; Shi, D.; Zhang, J.; Wang, M.; Jing, X.; Humphry-Baker, R.; Wang, P.; Zakeeruddin, S. M.; Grätzel, M. *J. Am. Chem. Soc.* **2008**, *130*, 10720.
(13) Chen, C. Y.; Chen, J. G.; Wu, S. J.; Li, J. Y.; Wu, C. G.; Ho, K. C. *Angew. Chem., Int. Ed.* **2008**, *47*, 7342.
(14) Gao, F.; Cheng, Y.; Yu, Q.; Liu, S.; Shi, D.; Li, Y.; Wang, P. *Inorg. Chem.* **2009**, *48*, 2664.
(15) Yin, J. F.; Bhattacharya, D.; Hsu, Y. C.; Tsai, C. C.; Lu, K. L.; Lin, H. C.; Chen, J. G.; Ho, K. C. *J. Mater. Chem.* **2009**, *19*, 7036.
(16) Robertson, N. *Angew. Chem., Int. Ed.* **2006**, *45*, 2338.
(17) Luo, Y. H.; Li, D. M.; Meng, Q. B. *Adv. Mater.* **2009**, *21*, 4647.
(18) Martinson, A. B. F.; Hamann, T. W.; Pellin, M. J.; Hupp, J. T. *Chem.—Eur. J.* **2008**, *14*, 4458.
(19) Zhang, Q. F.; Chou, T. P.; Russo, B.; Jenekhe, S. A.; Cao, G. Z. *Angew. Chem., Int. Ed.* **2008**, *47*, 2402.
(20) Jang, S.-R.; Lee, C.; Choi, H.; Ko, J. J.; Lee, J.; Vittal, R.; Kim, K.-J. *Chem. Mater.* **2006**, *18*, 5604.
(21) Kuang, D.; Klein, C.; Ito, S.; Moser, J.-E.; Humphry-Baker, R.; Evans, N.; Duriaux, F.; Grätzel, C.; Zakeeruddin, S. M.; Grätzel, M. *Adv. Mater.* **2007**, *19*, 1133.

 Published on Web 07/12/2010 

**Chart 1. Molecular Structures of JF-2, JF-5, JF-6, and JF-7**

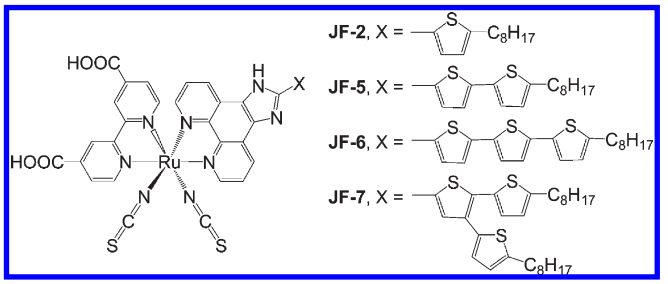


chromophores to enhance and broaden the MLCT band. However, this route also involves a decrease in the quantity of dye that can be loaded on the $TiO_2$ surface, because of the larger volume of dye molecules, a factor that lowers device performance.[23] Therefore, the issue arises as to what is the optimum length of oligothiophene antennas required to optimize these two inversely proportional factors and result in superior device performance. Herein, we report on an excellent resolution to this problem by a comparison of four ruthenium sensitizers, **JF-5**, **JF-6**, **JF-7** and **JF-2** (where **JF-2** has been reported in our previous study[15]), with ancillary ligands of linear or dendritic conjugated oligothiophene antennas (Chart 1). The power-conversion efficiencies of these dyes were optimized by incorporating a linear 2,2′-bithiophene antenna and this optimization can be explained by the experimental data collected and was further confirmed in theoretical studies. This finding not only optimizes the power-conversion efficiency in ruthenium sensitizers containing oligothiophene antennas but also represents an alternative strategy for improving DSCs.

## Results and Discussion

The 5-octyl-(2,2′-bithiophene) and 5-octyl-(2,2′,5′,2″-terthiophene) were obtained by forming the dianion of their oligothiophene precursors with 1.2 equiv of *n*-butyllithium, followed by reaction with 1-bromooctane. 5-Octyl-(2,2′-bithiophene)-5′-carbaldehyde and 5-octyl-(2,2′,5′,2″-terthiophene)-5″-carbaldehyde were prepared using the same synthetic procedure as described above, only *N*-formylpiperidine was used instead of 1-bromooctane. Coupling with 1,10-phenanthroline-5,6-dione and ammonium acetate as the source of ammonia in glacial acetic acid to form the ancillary ligands, obtip and ottip, according to protocols reported by Steck and Day.[25] The synthetic procedure for preparing dottip is very similar to that for obtip and ottip. The synthesis of the dottip ligand started by coupling 2,3-dibromothiophene and trimethyl(5-octylthiophen-2-yl)stannane via a Stille coupling, followed by a reaction with *N*-formylpiperidine and coupling with 1,10-phenanthroline-5,6-dione. Scheme 1 depicts the synthetic routes of the ancillary ligands, obtip, ottip and dottip. The ruthenium complexes, **JF-5**, **JF-6** and **JF-7**, were prepared by treating a ruthenium dimer with each of the ancillary ligands, i.e., obtip, ottip and dottip, respectively, in dimethylformamide (DMF) under an argon atmosphere using a typical one-pot synthesis.[26] The reaction of $[RuCl_2(p\text{-cymene})]_2$ with an ancillary ligand in a 1:2 stoichiometry in dry DMF at 80 °C resulted in the formation of a mononuclear Ru(II) complex. Afterward, the anchoring ligand (dcbpy, 4,4′-dicarboxylic acid-2,2′-bipyridine) was added, and the reaction mixture was refluxed in the dark. In this process, the cymene ligand from the Ru(II) coordination sphere is replaced by dcbpy. Finally, excess ammonium thiocyanate was added to afford the desired ruthenium sensitizers as reaction products.

The three new ruthenium sensitizers, [Ru(dcbpy)(obtip)(NCS)$_2$] (**JF-5**, dcbpy = 4,4′-dicarboxylic acid-2,2′-bipyridine, obtip = 2-(5-octyl-(2,2′-bithiophen)-5′-yl)-1*H*-imidazo-[4,5-*f*][1,10]phenanthroline), [Ru(dcbpy)(ottip)(NCS)$_2$] (**JF-6**, ottip = 2-(5-octyl-2,2′,5′,2″-terthiophen)-5″-yl)-1*H*-imidazo[4,5-*f*][1,10]phenanthroline), and [Ru(dcbpy)-(dottip)(NCS)$_2$] (**JF-7**, dottip = 2-(2,3-di-(5-octylthiophen-2-yl)thiophen-5-yl)-1*H*-imidazo[4,5-*f*][1,10]phenanthroline), were synthesized in a typical one-pot reaction. The UV−vis absorption spectra of the series of ruthenium sensitizers, **JF-5**, **JF-6**, and **JF-7**, in DMF solution consist of three main features, assigned as bands I, II and III with increasing energy order (Figure 1 and Table 1). Band III at 310 nm is assigned to the overlap of an intraligand $\pi-\pi^*$ transition. Band II, at around 358−430 nm, includes both intraligand $\pi-\pi^*$ and MLCT transitions. The molar extinction coefficient ($\varepsilon$) of the lower energy MLCT band I at 520 nm in **JF-6** is $1.49 \times 10^4$ $M^{-1}$ $cm^{-1}$, higher than that of **JF-5** and **JF-7**. This enhancement is because **JF-6** has a longer and planar oligothiophene main chain which not only increases the light-harvesting capability but also maintains the delocalized $\pi$-framework throughout entire molecule. Moreover, band II could be red-shifted and increased its $\varepsilon$ value, presumably due to the elongation of the length of the oligothiophene main chain. Although **JF-7** also contains three thiophene moieties, the bifurcated and twisted oligothiophene moiety destroys the connection of the delocalized $\pi$-framework in dottip (illustrated in Figure 3). For this reason, **JF-7** shows a lower MLCT intensity compared with the corresponding values for **JF-5** and **JF-6**. Therefore, it can be generally assumed that the MLCT intensity would increase by elongating rather than bifurcating the oligothiophene chain.

The electrochemical behaviors of the ruthenium dyes, **JF-5**, **JF-6**, and **JF-7**, were investigated by cyclic and square-wave voltammetry (Figure 2) and their oxidation potentials are listed in Table 1. The cyclic voltammograms showed that the oxidation and reduction potentials of all dyes are very close to each other. Moreover, the oxidation potentials of **JF-5**, **JF-6**, and **JF-7** were unequivocally

(22) Lee, C.; Yum, J.-H.; Choi, H.; Kang, S. O.; Ko, J.; Humphry-Baker, R.; Grätzel, M.; Nazeeruddin, M. K. *Inorg. Chem.* **2008**, *47*, 2267.
(23) Choi, H.; Baik, C.; Kim, S.; Kang, M.-S.; Xu, X.; Kang, H. S.; Kang, S. O.; Ko, J.; Nazeeruddin, M. K.; Grätzel, M. *New J. Chem.* **2008**, *32*, 2233.
(24) Sauvage, F.; Fischer, M. K. R.; Mishra, A.; Zakeeruddin, S. M.; Nazeeruddin, M. K.; Bäuerle, P.; Grätzel, M. *ChemSusChem* **2009**, *2*, 761.
(25) Steck, E. A.; Day, A. R. *J. Am. Chem. Soc.* **1943**, *65*, 452.
(26) Nazeeruddin, M. K.; Zakeeruddin, S. M.; Lagref, J.-J.; Liska, P.; Comte, P.; Barolo, C.; Viscardi, G.; Schenk, K.; Grätzel, M. *Coord. Chem. Rev.* **2004**, *248*, 1317.

**Scheme 1. Synthetic Procedure of the Ancillary Ligands, obtip, ottip and dottip [a]**

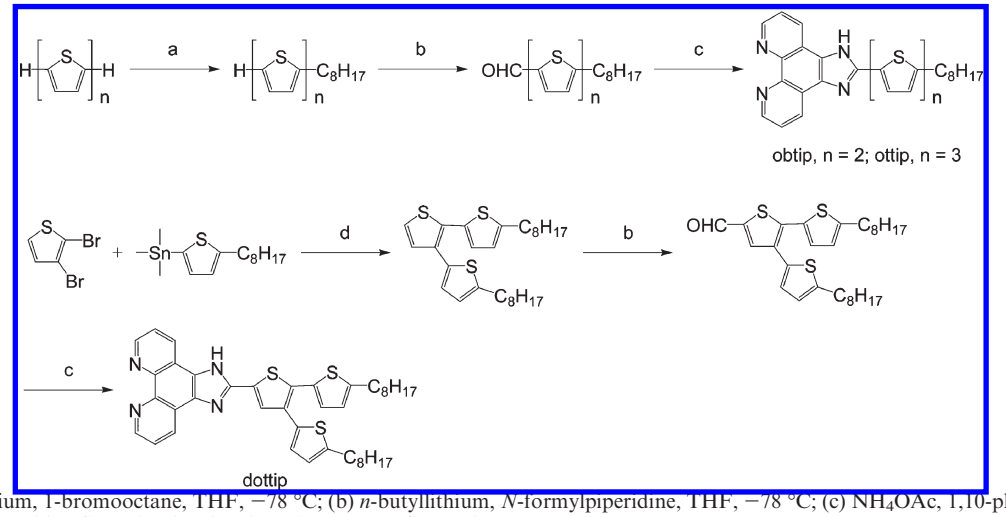


[a] (a) *n*-Butyllithium, 1-bromooctane, THF, −78 °C; (b) *n*-butyllithium, *N*-formylpiperidine, THF, −78 °C; (c) $NH_4OAc$, 1,10-phenanthroline-5,6-dione, glacial acetic acid, reflux 2 h; (d) $Pd(PPh_3)_2Cl_2$, DMF, reflux 22 h.

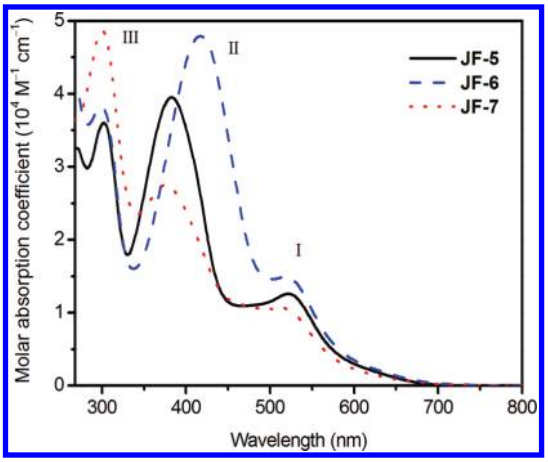


**Figure 1.** UV−vis absorption spectra of the series ruthenium sensitizers, **JF-5**, **JF-6**, and **JF-7** in DMF solution.

determined to be 0.30, 0.32, and 0.31 (V vs $Fc/Fc^+$) by square-wave voltammetry, respectively. The highest-occupied molecular orbitals (HOMOs) and lowest-unoccupied molecular orbitals (LUMOs) energy levels of all ruthenium dyes were calculated from their oxidation potentials and the absorption edge obtained from the UV−vis absorption spectra (Table 1 and Figure 3). These HOMO and LUMO energy levels, compared to the levels of the conduction band of $TiO_2$ and the redox electrolyte, are appropriate for electron injection and dye regeneration.

The optimized molecular structures for **JF-5**, **JF-6**, and **JF-7**, as well as the frontier molecular orbitals of their calculated HOMOs and LUMOs energy levels are shown in Figure 3. On closer inspection, the frontier molecular orbitals of **JF-5**, **JF-6**, and **JF-7** indicate that the HOMOs are localized on the mixed $Ru-t_{2g}$ and $NCS-\pi$ orbital. The LUMOs of these series ruthenium sensitizers are localized homogeneously on the anchoring ligand. The selected and calculated results of time dependent DFT (TDDFT) singlet excited-state transitions for MLCT band I of the series ruthenium sensitizers are listed in Table 2. Analyses of the transitions and orbital contributions indicate that band I of **JF-6** included a higher oscillator strength ($f$ = 0.1625) and a higher probability of MLCT transitions (72%) compared with that of **JF-5** ($f$ = 0.1171; 66%) and **JF-7** ($f$ = 0.1152; 57%). This result points out again that ruthenium sensitizers with longer and planar oligothiophene antenna have the ability to enhance MLCT intensity. The experimental and predicted electronic spectra are in overall good agreement.

Figure 4 shows the current density−voltage ($J-V$) characteristics and monochromatic incident photon-to-current conversion efficiency (IPCE) curves for the **JF-5**-, **JF-6**-, and **JF-7**-sensitized solar cells. The **JF-5**-sensitized solar cell gave a short-circuit photocurrent density ($J_{sc}$) of 18.3 mA $cm^{-2}$, an open-circuit voltage ($V_{oc}$) of 0.73 V and a fill factor ($ff$) of 0.71, which correspond to a surprisingly high overall power-conversion efficiency ($\eta$) of 9.5% compared with **JF-6** (8.7%), **JF-7** (6.4%), and **N3** (8.8%) under standard global AM 1.5 solar conditions (device data listed in Table 1). The calculated $J_{sc}$ from the overlap integral of the IPCE with the standard AM 1.5 solar emission spectrum is 17.0 mA $cm^{-2}$, and the mismatch factor[27] of the calculated and measured photocurrent density is less than 1.08. The values for $J_{sc}$ calculated by integration of the IPCE with the AM 1.5G solar spectrum for all dyes are listed in Table 1. Moreover, the IPCE curve for **JF-5** (as shown Figure 4) is over 80% in the 400−600 nm range, with the highest value of 92% at 523 nm compared with that of **JF-6** (84%) and **JF-7** (76%). The dye-loading measurement (listed in Table 1) indicated that **JF-5** contains a higher quantity of loaded dye ($1.8 \times 10^{-7}$ mol $cm^{-2}$), compared with that of **JF-6** ($1.1 \times 10^{-7}$ mol $cm^{-2}$) and **JF-7** ($0.5 \times 10^{-7}$ mol $cm^{-2}$). The decreasing dye-loading quantity in **JF-5** to **JF-7** is because of the increased volume of dye molecules, produced by further elongating or bifurcating the oligothiophene antenna.

Figure 5 shows the relationship between $\varepsilon$ for MLCT band I, $\Gamma$, and $\eta$ of **JF-2**,[15] **JF-5**, **JF-6**, and **JF-7**. Although

(27) Shrotriya, V.; Li, G.; Yao, Y.; Moriarty, T.; Emery, K.; Yang, Y. *Adv. Funct. Mater.* **2006**, *16*, 2016.

**Table 1. Optical, Electrochemical Data, and Cell Performance of JF-5, JF-6, and JF-7**

| | $\varepsilon$ ( $\times 10^4$ $M^{-1}$ $cm^{-1}$) | | | | | | cell performance[d] | | | | |
|---|---|---|---|---|---|---|---|---|---|---|---|
| dye | $\pi-\pi^*$ | $\pi-\pi^*$ or 4d$-\pi^*$ | 4d$-\pi^*$ | $E_{ox}$[b] of $Ru^{III/II}$ (V vs $Fc/Fc^+$) | $E_{HOMO}$[c] (eV) | $E_{LUMO}$[c] (eV) | $J_{sc}$ (mA $cm^{-2}$) | $V_{oc}$ (V) | *ff* | $\eta$ (%)[e] | $\Gamma$[f] ($\times 10^{-7}$ mol $cm^{-2}$) |
| **JF-5** | 3.59 (302)[a] | 3.95 (383) | 1.26 (520) | 0.30 | 5.40 | 3.66 | 18.3 (17.0)[g] | 0.73 | 0.71 | 9.5 | 1.8 |
| **JF-6** | 3.83 (299) | 4.79 (417) | 1.49 (520) | 0.32 | 5.42 | 3.70 | 17.0 (15.9) | 0.72 | 0.71 | 8.7 | 1.1 |
| **JF-7** | 4.87 (300) | 2.75 (375) | 1.05 (520) | 0.31 | 5.41 | 3.65 | 13.1 (12.5) | 0.70 | 0.70 | 6.4 | 0.5 |

[a] Absorption maxima, $\lambda_{max}$ (nm). [b] The $Ag/AgNO_3$ reference electrode was calibrated with a ferrocene/ferrocinium ($Fc/Fc^+$) redox couple. The electrochemical experiments were carried out in 0.1 M tetrabutylammonium tetrafluoroborate/DMF solution. [c] The values of $E_{HOMO}$ and $E_{LUMO}$ were calculated with the following formula: HOMO (eV) = $E_{ox} - E_{Fc/Fc+} + 5.1$; LUMO (eV) = HOMO $- E_g$. $E_g$ is the absorption onset estimated from the electronic absorption spectra of the sensitizers. [d] The cell performance data of **JF-5**, **JF-6**, and **JF-7** were the average of four measurements. [e] The power-conversion efficiency of **N3**-sensitized solar cell (where **N3** is $[Ru(dcbpy)_2(NCS)_2]$) measured by the same device fabrication process is 8.8%. [f] $\Gamma$ is the surface concentration of the dye molecules on $TiO_2$ film. [g] The values in parentheses were calculated by integration of the IPCE with the AM 1.5G solar spectrum.

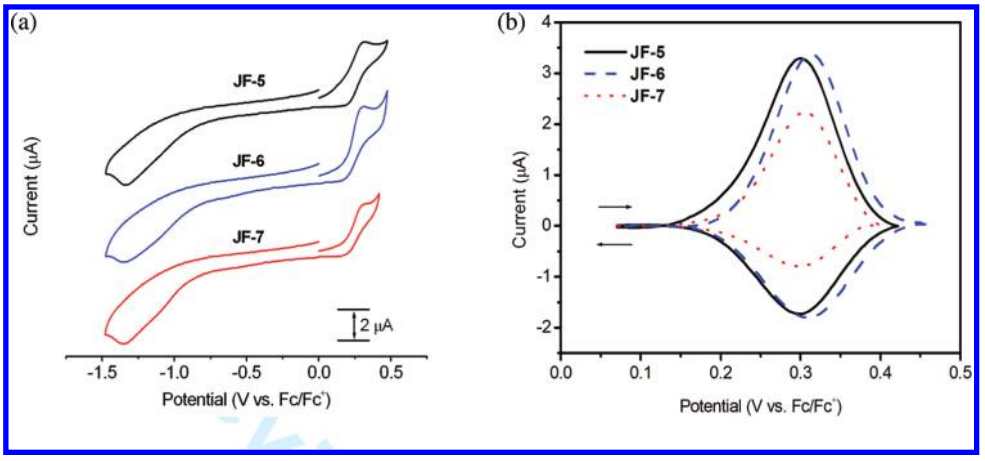


**Figure 2.** (a) Cyclic and (b) square-wave voltammograms of ruthenium sensitizers, **JF-5**, **JF-6**, and **JF-7**, in DMF.

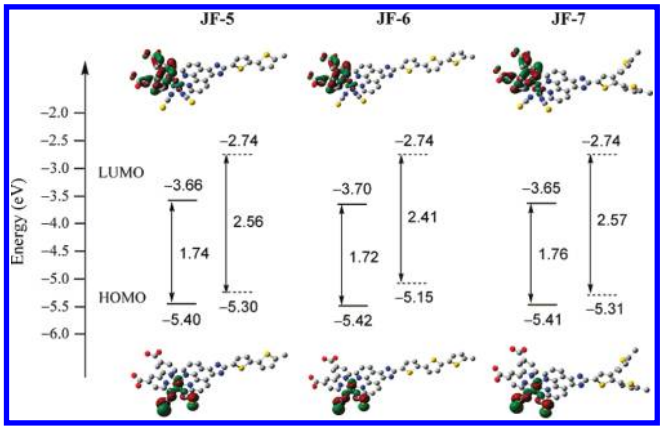


**Figure 3.** Schematic representation of the frontier orbitals of **JF-5**, **JF-6**, and **JF-7**, along with isodensity plots of the HOMO and LUMO orbitals. The experimental and calculated energy levels are displayed in solid and dashed line, respectively.

**JF-5** displayed the second highest MLCT intensity and dye-loading quantity, their curves intersect around **JF-5**, indicating that the oligothiophene antenna (2,2′-bithiophene) in **JF-5** is able to simultaneously acquire the best overall benefit from these two factors, resulting in the highest power-conversion efficiency.

Electrochemical impedance spectra (EIS) indicated that the DSCs consist of mainly three resistances, corresponding to three semicircles, which from first to third are the resistance of the charge transfer at the counter electrode,

**Table 2. Selected Results of Time Dependent DFT (TDDFT) Singlet Excited-State Transitions for MLCT Band I of JF-5, JF-6, and JF-7, Respectively, in Dimethylformamide**

| dye | wavelength (nm) | *f* | major contribution |
|---|---|---|---|
| **JF-5** | 672.8 | 0.0239 | HOMO → LUMO (79%) |
| | 595.9 | 0.0006 | HOMO−3 → LUMO (67%) |
| | 548.6 | 0.1171 | HOMO−2 → LUMO (66%) |
| | 523.8 | 0.0034 | HOMO−1 → LUMO (73%) |
| **JF-6** | 672.3 | 0.0237 | HOMO−1 → LUMO (86%) |
| | 597.2 | 0.0006 | HOMO−2 → LUMO (71%) |
| | 564.2 | 0.0003 | HOMO → LUMO (79%) |
| | 548.1 | 0.1625 | HOMO−3 → LUMO (72%) |
| **JF-7** | 671.1 | 0.0233 | HOMO → LUMO (85%) |
| | 594.4 | 0.0006 | HOMO−3 → LUMO (58%) |
| | 547.4 | 0.1152 | HOMO−2 → LUMO (57%) |
| | 514.2 | 0.0005 | HOMO−1 → LUMO (80%) |

the resistance at the dye-adsorbed $TiO_2$/electrolyte interface together with electron transport in the $TiO_2$ network, and the resistance of triiodide to diffusion in the electrolyte, respectively.[28−31] It is clear from Figure 6 that the

(28) Wang, Q.; Moser, J.-E.; Grätzel, M. *J. Phys. Chem. B* **2005**, *109*, 14945.
(29) Kroon, J. M.; Bakker, N. J.; Smit, H. J. P.; Liska, P.; Thampi, K. R.; Wang, P.; Zakeeruddin, S. M.; Grätzel, M.; Hinsch, A.; Hore, S.; Würfel, U.; Sastrawan, R.; Durrant, J. R.; Palomares, E.; Pettersson, H.; Gruszecki, T.; Walter, J.; Skupien, K.; Tulloch, G. E. *Prog. Photovolt: Res. Appl.* **2007**, *15*, 1.
(30) Wang, Q.; Ito, S.; Grätzel, M.; Fabregat-Santiago, F.; Mora-Seró, I.; Bisquert, J.; Bessho, T.; Imai, H. *J. Phys. Chem. B* **2006**, *110*, 25210.
(31) Wang, Q.; Zhang, Z.; Zakeeruddin, S. M.; Grätzel, M. *J. Phys. Chem. C* **2008**, *112*, 7084.

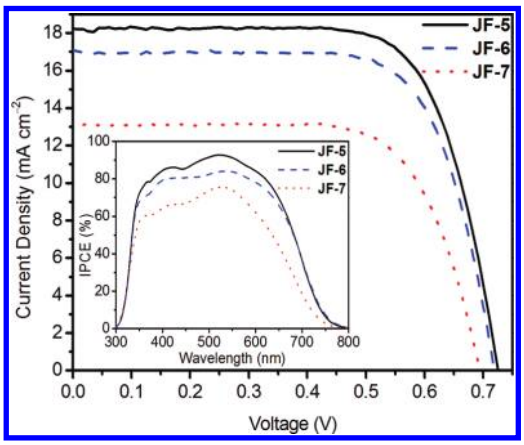


**Figure 4.** Current density−voltage characteristics of the photovoltaic devices with **JF-5**, **JF-6**, and **JF-7** as photosensitizers under AM 1.5 simulated sunlight (100 mW cm$^{-2}$) illumination. (thickness of $TiO_2$ = 12 $\mu$m; cell active area = 0.16 cm$^2$); inset: the incident photon-to-current conversion efficiency spectra of the photovoltaic devices with different photosensitizers.

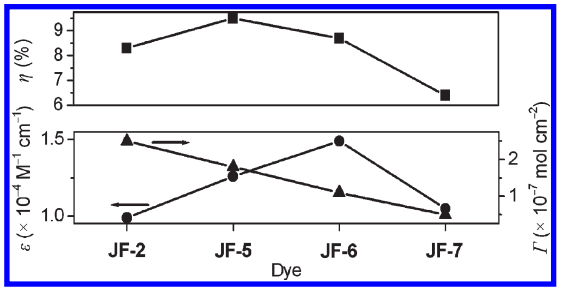


**Figure 5.** Variation in the optical, dye-loading properties and power-conversion efficiencies for **JF-2**, **JF-5**, **JF-6**, and **JF-7**.

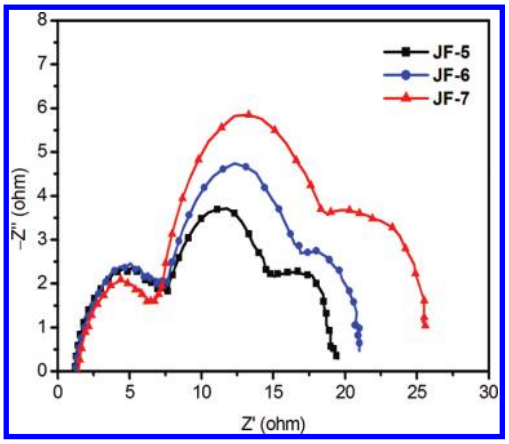


**Figure 6.** Electrochemical impedance spectra of **JF-5**-, **JF-6**-, and **JF-7**-sensitized solar cells in the form of a Nyquist plot.

radii of the second semicircles increase in the order **JF-5** < **JF-6** < **JF-7**. This indicates that the overall resistance at the $TiO_2$/electrolyte interface and $TiO_2$ network of the **JF-5**-sensitized solar cell is smaller than that for the **JF-6**- and **JF-7**-sensitized solar cells. An EIS analysis also supports the conclusion that device performance of **JF-5** is superior. Therefore, the **JF-5**-sensitized solar cell exhibits the best overall device performance, as compared to that of the **JF-2**-, **JF-6**-, and **JF-7**-sensitized solar cells. This optimization of power-conversion efficiency by varying the length of the light-harvesting oligothiophene antenna can be explained by UV−vis absorption spectra, electrochemical data, dye-loading measurements, electrochemical impedance spectroscopy (EIS), density functional theory (DFT), and time-dependent density functional theory (TDDFT) studies.

## Conclusion

In conclusion, we report on the design and synthesis of three new ruthenium sensitizers, **JF-5**, **JF-6**, and **JF-7**, with excellent power-conversion efficiency and optimize the light-harvesting oligothiophene antennas that contain 2,2′-bithiophene, which shows superior device performance. The difference in the performance of these sensitizers demonstrates that elongating the linear and planar light-harvesting antenna result in an enhancement in MLCT intensity, but a reduction in the quantity of dye-loading. Moreover, the sensitizer incorporating a longer ancillary ligand employed in DSCs would result in an increased cell resistance. This finding not only permitted the power-conversion efficiency in ruthenium sensitizers containing oligothiophene antennas to be optimized, but also points to a promising direction for molecule engineering in DSCs.

## Experimental Section

**Materials and Measurements.** All reactants and solvents were purchased from commercial sources and used as received. $^1$H NMR spectra were recorded on a Bruker AMX400 or AV400 spectrometer with tetramethylsilane as the internal standard. Elemental analysis was determined on a Perkin-Elmer 2400 CHN analyzer. Mass spectrometry was performed with a JMS-700 double focusing mass spectrometer (JEOL, Tokyo, Japan). Absorption spectra were recorded with a UV−vis spectrophotometer (Hewlett-Packard 8453). Cyclic and square-wave voltammetry were performed on a CH Instruments electrochemical analyzer in DMF solutions ($10^{-3}$ M) with a platinum plate as the working electrode, a platinum wire auxiliary electrode, and a nonaqueous $Ag/AgNO_3$ reference electrode. The supporting electrolyte was tetrabutylammonium tetrafluoroborate (0.1 M), and ferrocene was selected as the internal standard. The solutions were bubbled with $N_2$ for 10 min before measurements. The scan rate for CV was 100 mV s$^{-1}$. The square-wave voltammograms swept with potential step increment of 10 mV and frequency of 25 Hz. The dye loading measurement on $TiO_2$ films was carried out by desorbing the dye into 0.1 M NaOH solution in $CH_3OH$ and then measuring the ultraviolet−visible absorption spectra of the resultant solution with the same dilution. The adsorbed quantity of each dye was calculated from the difference in concentration for each solution before and after $TiO_2$ film immersion. Electrochemical impedance spectra (EIS) of the DSCs were obtained using a potentiostat/galvanostat equipped with FRA2 modules under a constant light illumination of 100 mW/cm$^2$ and the frequency range used was from 10 mHz to 65 kHz. The applied bias voltage and ac amplitude were set at the open-circuit voltage ($V_{oc}$) of the DSCs and 10 mV, respectively.

**5-Octyl-(2,2′-bithiophene)-5′-carbaldehyde.** The precursor, 5-octyl-(2,2′-bithiophene), was synthesized by previously reported procedures.[8] 5-Octyl-(2,2′-bithiophene) (277.5 mg, 1.0 mol) was dissolved in 30 mL THF in a well-dried flask under the protection of a $N_2$ flow. The solution was cooled in a liquid nitrogen/acetone cooling bath, and *n*-butyllithium (0.8 mL, 1.28 mmol, 1.6 M

in hexane) was then added dropwise. The cooling bath was removed, and the solution was allowed to warm to room temperature and *N*-formylpiperidine (139.8 mg, 1.2 mmol) was then added in one portion. After 6 h, the solution was poured into 200 mL of cool water. The organic layer was separated, and the aqueous layer was extracted with ether. The organic layers were collected, dried over anhydrous $MgSO_4$, and the removal of the solvent gave the crude product. The crude product was purified by chromatography using $CH_2Cl_2$/hexane (1:1) as the eluent to afford 239.1 mg (0.78 mmol, yield 78.0%) of 5-octyl-(2,2′-bithiophene)-5′-carbaldehyde as light yellow liquid. $^1$H NMR ($CD_2Cl_2$, 400 MHz) $\delta$ ppm: 9.86 (s, 1H), 7.69 (d, $J$ = 4.0 Hz, 1H), 7.24 (d, $J$ = 3.6, 1H), 7.22 (d, $J$ = 4.0, 1H), 6.82 (d, $J$ = 3.6, 1H), 2.82 (t, 2H), 1.68 (m, 2H), 1.34 (m, 10H), 0.95 (t, 3H). EI-MS ($m/z$): 306.2 $[M]^+$.

**2-(5-Octyl-(2,2′-bithiophen)-5′-yl)-1*H*-imidazo[4,5-*f*][1,10]phenanthroline (obtip).** A mixture of 1,10-phenanthroline-5,6-dione (254.3 mg, 1.2 mmol), 5-octyl-(2,2′-bithiophen)-2′-carbaldehyde (306.7 mg, 1.0 mmol), ammonium acetate (1548.9 mg, 20.2 mmol), and glacial acetic acid (30 mL) was refluxed for 2 h. After the reaction, the mixture was poured into 200 mL of cool water, and the resulting precipitate was isolated by filtration. The crude products were washed with water and purified by chromatography using $CH_2Cl_2$/hexane/MeOH (5:5:2) as the eluent to afford 2-(5-octyl-(2,2′-bithiophen)-5′-yl)-1*H*-imidazo[4,5-*f*][1,10]phenanthroline (362.1 mg, 0.729 mmol, 73%) as brown solid, mp 198 °C. $^1$H NMR ([$D_6$] DMSO, 300 MHz) $\delta$ ppm: 9.03 (d, $J$ = 1.2 Hz, 2H), 8.83 (d, $J$ = 7.8 Hz, 2H), 7.82 (m, 3H), 7.33 (d, $J$ = 3.9 Hz, 1H), 7.26 (d, $J$ = 3.6 Hz, 1H), 6.85 (d, $J$ = 3.6 Hz, 1H), 2.79 (t, $J$ = 7.4 Hz, 2H), 1.61 (m, 2H), 1.24 (m, 10H), 0.83 (t, $J$ = 6.6 Hz, 3H). EI-MS ($m/z$): 496.2 $[M]^+$.

**[Ru(dcbpy)(obtip)(NCS)$_2$] (JF-5).** [$RuCl_2$(p-cymene)]$_2$ (306.3 mg, 0.5 mmol) and obtip (500.3 mg, 1.0 mmol) were added to dry DMF (20 mL). The reaction mixture was heated at 80 °C under $N_2$ for 4 h, and then dcbpy (4,4′-dicarboxylic acid-2,2′-bipyridine; 244.0 mg, 1 mmol) was added. The reaction mixture was refluxed at 160 °C for another 4 h in the dark. Excess $NH_4NCS$ was added to the reaction mixture and heated at 130 °C for 5 h. After the reaction, the solvent was removed by rotary evaporator. The product was collected and washed with water and diethyl ether. The crude product was dissolved in methanol then passed through a column using methanol as the eluent. The main band was collected and concentrated, 335.3 mg (0.349 mmol, 35%) of black solid was obtained, mp > 400 °C. $^1$H NMR ([$D_6$] DMSO, 400 MHz) $\delta$ ppm: 9.53 (m, 2H), 9.11 (m, 2H), 8.93 (s, 1H), 8.71 (d, $J$ = 8.1 Hz, 1H), 8.35 (m, 2H), 7.88 (d, $J$ = 3.3 Hz, 1H), 7.83 (d, $J$ = 4.8 Hz, 1H), 7.68 (d, $J$ = 5.7 Hz, 1H), 7.59 (t, $J$ = 6.5 Hz, 1H), 7.47 (d, $J$ = 4.5 Hz, 1H), 7.34 (d, $J$ = 3.6 Hz, 1H), 7.26 (d, $J$ = 3.3 Hz, 1H), 6.85 (d, $J$ = 3.3 Hz, 1H), 2.78 (t, $J$ = 7.2 Hz, 2H), 1.53 (t, $J$ = 7.2 Hz, 2H), 1.28 (m, 10H), 0.85 (t, $J$ = 5.4 Hz, 3H). FAB-MS ($m/z$): 900.4 $[M - NCS]^+$. Anal. Calcd for $C_{43}H_{36}N_8O_4RuS_4$: C 53.90, H 3.79, N 11.70, S 13.39. Found: C 53.72, H 3.86, N 11.49, S 12.98.

**5-Octyl-(2,2′,5′,2″-terthiophene).** The precursor, 2,2′,5′,2″-terthiophene, was synthesized by previously reported procedures.[32] 2,2′,5′,2″-Terthiophene (247.6 mg, 1.0 mmol) was dissolved in 30 mL THF in a well-dried flask under the protection of a $N_2$ flow. The solution was cooled in a liquid nitrogen/acetone cooling bath, and *n*-butyllithium (0.8 mL, 1.28 mmol, 1.6 M in hexane) was then added dropwise. The cooling bath was removed, and the solution was allowed to warm to room temperature and 1-bromooctane (219.8 mg, 1.1 mmol) was then added in one portion. After 6 h, the solution was poured into 200 mL of cool water. The organic layer was separated, and the aqueous layer was extracted with ether. The organic layers were collected, dried over anhydrous $MgSO_4$, and the removal of the solvent gave the crude product. The crude product was purified by chromatography using hexane as the eluent to afford 183.8 mg (0.51 mmol, yield 51%) of 5-octyl-(2,2′,5′,2″-terthiophene) as light yellow solid, mp 69 °C. $^1$H NMR ($CDCl_3$, 400 MHz) $\delta$ ppm: 7.18 (d, $J$ = 5.2 Hz, 1H), 7.13 (d, $J$ = 3.2 Hz, 1H), 7.03 (d, $J$ = 4.0 Hz, 1H), 6.97 (m, 3H), 6.66 (d, $J$ = 3.2 Hz, 1H), 2.77 (t, $J$ = 7.6 Hz, 2H), 1.66 (m, 2H), 1.27 (m, 10H), 0.86 (t, $J$ = 6.8 Hz, 3H). FAB-MS ($m/z$): 360.1 $[M]^+$.

**5-Octyl-(2,2′,5′,2″-terthiophene)-5″-carbaldehyde.** 5-Octyl-(2,2′,-5′,2″-terthiophene) (361.3 mg, 1.0 mmol) was dissolved in 30 mL THF in a well-dried flask under the protection of a $N_2$ flow. The solution was cooled in a liquid nitrogen/acetone cooling bath, and *n*-butyllithium (0.8 mL, 1.28 mmol, 1.6 M in hexane) was then added dropwise. The cooling bath was removed, and the solution was allowed to warm to room temperature and *N*-formylpiperidine (132.3 mg, 1.2 mmol) was then added in one portion. After 6 h, the solution was poured into 200 mL of cool water. The organic layer was separated, and the aqueous layer was extracted with ether. The organic layers were collected and dried over anhydrous $MgSO_4$, and the removal of the solvent gave the crude product. The crude product was purified by chromatography using $CH_2Cl_2$/hexane (1:1) as the eluent to afford 285.5 mg (0.73 mmol, yield 73%) of 5-octyl-(2,2′,5′,2″-terthiophene)-5″-carbaldehyde as yellow solid, mp 90 °C. $^1$H NMR ($CD_2Cl_2$, 400 MHz) $\delta$ ppm: 9.82 (s, 1H), 7.65 (d, $J$ = 3.6 Hz, 1H), 7.26 (d, $J$ = 4.0 Hz, 1H), 7.22 (d, $J$ = 4.0 Hz, 1H), 7.05 (d, $J$ = 1.2 Hz, 1H), 7.04 (d, $J$ = 1.2 Hz, 1H), 6.71(d, $J$ = 3.6 Hz, 1H), 2.79 (t, $J$ = 8.0 Hz, 2H), 1.67 (m, 2H), 1.27 (m, 10H), 0.88 (t, $J$ = 6.8 Hz, 3H). FAB-MS ($m/z$): 389.1 $[M + H]^+$.

**2-(5-Octyl-(2,2′,5′,2″-terthiophen)-5″-yl)-1*H*-imidazo[4,5-*f*]-[1,10]phenanthroline (ottip).** A mixture of 1,10-phenanthroline-5,6-dione (221.0 mg, 1.1 mmol), 5-octyl-(2,2′,5′,2″-terthiophene)-5′-carbaldehyde (388.3 mg, 1.0 mmol), ammonium acetate (1553.2 mg, 20.2 mmol), and glacial acetic acid (30 mL) was refluxed for 2 h. After the reaction, the mixture was poured into 200 mL of cool water, and the resulting precipitate was isolated by filtration. The crude products were washed with water and purified by chromatography using $CH_2Cl_2$/hexane/MeOH (5:5:2) as the eluent to afford 2-(5-octyl-2,2′,5′,2″-terthiophen)-5″-yl)-1*H*-imidazo[4,5-*f*][1,10]phenanthroline (437.9 mg, 0.76 mmol, 76%) as brown solid, mp 223 °C. $^1$H NMR ([$D_6$] DMSO, 400 MHz) $\delta$ ppm: 9.04 (d, $J$ = 3.6 Hz, 2H), 8.86 (s, 2H), 7.84 (m, 3H), 7.45 (d, $J$ = 3.6 Hz, 1H), 7.40 (d, $J$ = 3.6 Hz, 1H), 7.22 (d, $J$ = 3.6 Hz, 1H), 7.17 (d, $J$ = 3.2 Hz, 1H), 6.82 (d, $J$ = 3.2 Hz, 1H), 2.78 (t, $J$ = 7.6 Hz, 2H), 1.61 (m, 2H), 1.24 (m, 10H), 0.85 (t, $J$ = 6.4 Hz, 3H). FAB-MS ($m/z$): 579.2 $[M + H]^+$.

**[Ru(dcbpy)(ottip)(NCS)$_2$] (JF-6).** [$RuCl_2$(p-cymene)]$_2$ (306.5 mg, 0.5 mmol) and ottip (580.4 mg, 1.0 mmol) were added to dry DMF (20 mL). The reaction mixture was heated at 80 °C under $N_2$ for 4 h and then dcbpy (4,4′-dicarboxylic acid-2,2′-bipyridine; 244.4 mg, 1.0 mmol) was added. The reaction mixture was refluxed at 160 °C for another 4 h in the dark. Excess $NH_4NCS$ was added to the reaction mixture and heated at 130 °C for 5 h. After the reaction, the solvent was removed by rotary evaporator. The product was collected and washed with water and diethyl ether. The crude product was dissolved in methanol then passed through a column using methanol as the eluent. The main band was collected and concentrated; 298.3 mg (0.29 mmol, 29%) of black solid was obtained, mp > 400 °C. $^1$H NMR ([$D_6$] DMSO, 400 MHz) $\delta$ ppm: 9.53 (m, 2H), 9.09 (m, 2H), 8.90 (s, 1H), 8.72 (d, $J$ = 5.2 Hz 1H), 8.35 (m, 2H), 7.89 (d, $J$ = 8.4 Hz, 1H), 7.83 (d, $J$ = 5.4 Hz, 1H), 7.68 (d, $J$ = 5.2 Hz, 1H), 7.60 (d, $J$ = 4.8 Hz,

(32) Leriche, P.; Aillerie, D.; Roquet, S.; Allain, M.; Cravino, A.; Frère, P.; Roncali, J. *Org. Biomol. Chem.* **2008**, *6*, 3202.

1H), 7.46 (m, 2H), 7.40 (d, $J$ = 3.8 Hz, 1H), 7.20 (d, $J$ = 3.8 Hz, 1H), 7.16 (d, $J$ = 3.4 Hz, 1H), 6.81 (d, $J$ = 3.4 Hz, 1H), 2.76 (t, $J$ = 6.8 Hz, 2H), 1.58 (m, 2H), 1.25 (m, 10H), 0.84 (t, $J$ = 6.8 Hz, 3H). FAB-MS ($m/z$): 1040.2 $[M]^+$. Anal. Calcd for $C_{47}H_{38}N_8O_4RuS_5$: C 54.27, H 3.68, N 10.77, S 15.41. Found: C 54.67, H 4.06, N 10.83, S 15.11.

**2,3-Di-(5-octylthiophen-2-yl)thiophene.** The precursor, trimethyl(5-octylthiophen-2-yl)stannane, was synthesized by previously reported procedures.[9] 2,3-Dibromothiophene (240.3 mg, 1.0 mmol) and trimethyl(5-octylthiophen-2-yl)stannane (810.8 mg, 2.3 mmol) were dissolved in 30 mL anhydrous DMF then $Pd(PPh_3)_2Cl_2$ (35.5 mg, 0.051 mmol) was added as a catalyst. The mixture was refluxed under $N_2$ for 22 h. After the mixture was cooled to room temperature, 5 wt % $NH_4Cl_{(aq)}$ was added to terminate the reaction and the product was extracted with $CH_2Cl_2$. The organic layer was washed with saturated $NaHCO_{3(aq)}$, distilled water and saturated $NaCl_{(aq)}$, respectively. The crude product was purified by chromatography using hexane as the eluent to afford 353.4 mg (0.747 mmol, 75%) of 2,3-di-(5-octylthiophen-2-yl)thiophene as yellow liquid. $^1$H NMR ($CDCl_3$, 400 MHz) $\delta$ ppm: 7.25 (d, $J$ = 5.2 Hz, 1H), 7.19 (d, $J$ = 5.2 Hz, 1H), 7.02 (d, $J$ = 3.6 Hz, 1H), 6.95 (d, $J$ = 3.6 Hz, 1H), 6.75 (d, $J$ = 4.0 Hz, 1H), 6.73 (d, $J$ = 4.0 Hz, 1H), 2.85 (m, 4H), 1.75 (m, 4H), 1.43 (m, 20H), 0.97 (m, 6H). EI-MS ($m/z$): 472.3 $[M]^+$.

**2,3-Di-(5-octylthiophen-2-yl)thiophene-5-carbaldehyde.** 2,3-Di-(5-octylthiophen-2-yl)thiophene (470.8 mg, 1.0 mmol) was dissolved in 30 mL THF in a well-dried flask under the protection of a $N_2$ flow. The solution was cooled in a liquid nitrogen/acetone cooling bath, and *n*-butyllithium (0.8 mL, 1.28 mmol, 1.6 M in hexane) was then added dropwise. The cooling bath was removed, and the solution was allowed to warm to room temperature and *N*-formylpiperidine (140.3 mg, 1.2 mmol) was then added in one portion. After 6 h, the solution was poured into 200 mL of cool water. The organic layer was separated, and the aqueous layer was extracted with ether. The organic layers were collected, washed with water, and dried over anhydrous $MgSO_4$, and the removal of the solvent gave the crude product. The crude product was purified by chromatography using $CH_2Cl_2$/hexane (1:1) as the eluent to afford 341.2 mg (0.681 mmol, yield 68%) of 2,3-di-(5-octylthiophen-2-yl)thiophene-5-carbaldehyde as yellow liquid. $^1$H NMR ($CDCl_3$, 400 MHz) $\delta$ ppm: 9.86 (s, 1H), 7.70 (s, 1H), 7.10 (d, $J$ = 3.6 Hz, 1H), 6.92 (d, $J$ = 3.6 Hz, 1H), 6.74 (d, $J$ = 3.6 Hz, 1H), 6.71(d, $J$ = 3.6 Hz, 1H), 2.82 (m, 4H), 1.68 (m, 4H), 1.29 (m, 20H), 0.89 (m, 6H). EI-MS ($m/z$): 500.3 $[M]^+$.

**2-(2,3-Di-(5-octylthiophen-2-yl)thiophen-5-yl)-1*H*-imidazo[4,5-*f*][1,10]phenanthroline (dottip).** A mixture of 1,10-phenanthroline-5,6-dione (229.5 mg, 1.1 mmol), 2,3-di-(5-octylthiophen-2-yl)thiophene-5-carbaldehyde (510.3 mg, 1.0 mmol), ammonium acetate (1632.5 mg, 21.2 mmol) and glacial acetic acid (30 mL) was refluxed for 2 h. After the reaction, the mixture was poured into 200 mL of cool water and the resulting precipitate was isolated by filtration. The crude products were washed with water and purified by chromatography using $CH_2Cl_2$/hexane/MeOH (5:5:2) as the eluent to afford 2-(2,3-di-(5-octylthiophen-2-yl)-thiophen-5-yl)-1*H*-imidazo[4,5-*f*][1,10]phenanthroline (456.3 mg, 0.66 mmol, 65%) as brown solid, mp 208 °C. $^1$H NMR ([$D_6$] DMSO, 400 MHz) $\delta$ ppm: 9.01 (d, $J$ = 3.2 Hz, 2H), 8.85 (d, $J$ = 8.4 Hz, 2H), 7.92 (s, 1H), 7.77 (dd, $J$ = 3.2, 8.4 Hz, 2H), 7.09 (d, $J$ = 3.6 Hz, 1H), 7.00 (d, $J$ = 3.6 Hz, 1H), 6.79 (d, $J$ = 3.2 Hz, 1H), 6.77 (d, $J$ = 3.2 Hz, 1H), 2.77 (m, 4H), 1.62 (m, 4H), 1.27 (m, 20H), 0.86 (m, 6H). EI-MS ($m/z$): 690.4 $[M]^+$.

**[Ru(dcbpy)(dottip)(NCS)$_2$] (JF-7).** $[RuCl_2(p\text{-cymene})]_2$ (306.0 mg, 0.5 mmol) and dottip (692.8 mg, 1.0 mmol) were added to dry DMF (20 mL). The reaction mixture was heated at 80 °C under $N_2$ for 4 h and then dcbpy (4,4′-dicarboxylic acid-2,2′-bipyridine; 244.9 mg, 1.0 mmol) was added. The reaction mixture was refluxed at 160 °C for another 4 h in the dark. Excess $NH_4NCS$ was added to the reaction mixture and heated at 130 °C for 5 h. After the reaction, the solvent was removed by rotary evaporator. The product was collected and washed with water and diethyl ether. The crude product was dissolved in methanol then passed through a column using methanol as the eluent. The main band was collected and concentrated, 380.2 mg (0.329 mmol, 33%) of black solid was obtained, mp > 400 °C. $^1$H NMR ([$D_6$] DMSO, 400 MHz) $\delta$ ppm: 9.57 (d, $J$ = 6.0 Hz, 1H), 9.53 (d, $J$ = 4.8 Hz, 1H), 9.20 (s, 1H), 9.07 (s, $J$ = 7.6 Hz, 1H), 8.98 (s, 1H), 8.72 (dd, $J$ = 8.4, 5.2 Hz, 1H), 8.39 (m, 2H), 7.99 (d, $J$ = 5.2 Hz, 1H), 7.86 (d, $J$ = 4.4 Hz, 1H), 7.75 (d, $J$ = 4.8 Hz, 1H), 7.62 (d, $J$ = 5.2 Hz, 1H), 7.50 (d, $J$ = 4.8 Hz, 1H), 7.17 (d, $J$ = 6.0 Hz, 1H), 7.09 (d, $J$ = 5.2 Hz, 1H), 6.86 (m, 2H), 2.78 (m, 2H), 1.60 (m, 2H), 1.24 (m, 10H), 0.85 (t, $J$ = 3.2 Hz, 3H). FAB-MS ($m/z$): 1094.4 $[M - NCS]^+$. Anal. Calcd for $C_{55}H_{54}N_8O_4RuS_5$: C 57.32, H 4.72, N 9.72, S 13.91. Found: C 56.88, H 5.16, N 9.30, S 13.14.

**Molecular Modeling.** The geometrical and electrochemical properties of the dye, **JF-5**, **JF-6**, and **JF-7**, were studied with density functional theory (DFT) and time-dependent density functional theory (TDDFT) calculations using Gaussian 03 (G03) program package,[33] employing the DFT method with Becke's three-parameter hybrid function[34] and Lee−Yang−Parr's gradient corrected correlation function[35] (B3LYP). The LanL2DZ effective core potential[36] was used for the ruthenium atom and the split-valence 6-31G** basis set[37] was applied for hydrogen, sulfur, carbon, oxygen and nitrogen atoms. The ground-state geometries of the dye molecules were optimized in the gas phase. Molecular orbitals were visualized using "Gauss View 3.09". TDDFT calculations for **JF-5**, **JF-6**, and **JF-7** were performed using the conductor-like polarizable continuum model method (C−PCM)[38−40] with dimethylformamide (DMF) as the solvent.[41] The empirical solvent data, molecular radius and dielectric constant ($\varepsilon$), employed in C−PCM are 2.647 Å and 36.71, respectively. Ninety singlet excited states were determined starting from geometry-optimized structures of **JF-5**, **JF-6**, and **JF-7**. The GaussSum 1.05[42] was used for analyzing the data of singlet excited-state transitions.

(33) Frisch, M. J.; Trucks, G. W.; Schlegel, H. B.; Scuseria, G. E.; Robb, M. A.; Cheeseman, J. R.; Montgomery, J. A.; Vreven, Jr., T.; Kudin, K. N.; Burant, J. C.; Millam, J. M.; Iyengar, S. S.; Tomasi, J.; Barone, V.; Mennucci, B.; Cossi, M.; Scalmani, G.; Rega, N.; Petersson, G. A.; Nakatsuji, H.; Hada, M.; Ehara, M.; Toyota, K.; Fukuda, R.; Hasegawa, J.; Ishida, M.; Nakajima, T.; Honda, Y.; Kitao, O.; Nakai, H.; Klene, M.; Li, X.; Knox, J. E.; Hratchian, H. P.; Cross, J. B.; Bakken, V.; Adamo, C.; Jaramillo, J.; Gomperts, R.; Stratmann, R. E.; Yazyev, O.; Austin, A. J.; Cammi, R.; Pomelli, C.; Ochterski, J.; Ayala, P. Y.; Morokuma, K.; Voth, G. A.; Salvador, P.; Dannenberg, J. J.; Zakrzewski, V. G.; Dapprich, S.; Daniels, A. D.; Strain, M. C.; Farkas, O.; Malick, D. K.; Rabuck, A. D.; Raghavachari, K.; Foresman, J. B.; Ortiz, J. V.; Cui, Q.; Baboul, A. G.; Clifford, S.; Cioslowski, J.; Stefanov, B. B.; Liu, G.; Liashenko, A.; Piskorz, P.; Komaromi, I.; Martin, R. L.; Fox, D. J.; Keith, T.; Al-Laham, M. A.; Peng, C. Y.; Nanayakkara, A.; Challacombe, M.; Gill, P. M. W.; Johnson, B. G.; Chen, W.; Wong, M. W.; Gonzalez, C.; Pople, J. A. *GAUSSIAN 03*, revision D.01, Gaussian Inc.: Wallingford, CT, 2004.
(34) Becke, A. D. *J. Chem. Phys.* **1993**, *98*, 5648.
(35) Lee, C.; Yang, W.; Parr, R. G. *Phys. Rev. B* **1988**, *37*, 785.
(36) Hay, P. J.; Wadt, W. R. *J. Chem. Phys.* **1985**, *82*, 270.
(37) McLean, A. D.; Chandler, G. S. *J. Chem. Phys.* **1980**, *72*, 5639.
(38) Cossi, M.; Rega, N.; Scalmani, G.; Barone, V. *J. Comput. Chem.* **2003**, *24*, 669.
(39) Cossi, M.; Barone, V. *J. Chem. Phys.* **2001**, *115*, 4708.
(40) Barone, V.; Cossi, M. *J. Phys. Chem. A* **1998**, *102*, 1995.
(41) Böes, E. S.; Livotto, P. R.; Stassen, H. *Chem. Phys.* **2006**, *331*, 142.
(42) O'Boyle, N. M.; Vos, J. G. *GaussSum 1.0*; Dublin City University: Dublin, Ireland, 2005; available at http://gausssum.sourceforge.net.

**Preparation of $TiO_2$ Electrode.** The preparation of the $TiO_2$ precursor and the electrode fabrication were carried out based on previous reports.[8,43] The $TiO_2$ film, serving as the photoanode in this work, was prepared through the general sol−gel method. The precursor solution was prepared according to the following procedure: To 430 mL of 0.1 M nitric acid solution under vigorous stirring, 72 mL of $Ti(C_3H_7O)_4$ slowly added dropwise to form a mixture. After hydrolysis, the mixture was heated at 85 °C in a water bath and stirred vigorously for 8 h to achieve peptization. When the mixture was cooled to room temperature, the resultant colloid was filtered, and then heated in an autoclave at a temperature of 240 °C for 12 h to grow the $TiO_2$ particles. After the colloid was cooled to room temperature, it was ultrasonically vibrated for 10 min. The $TiO_2$ colloid was concentrated to 13 and 30 wt % (with respect to $TiO_2$ weight) of poly(ethylene glycol) (PEG, MW = 20 000 and 200 000), which was added to prevent the film from cracking during drying. To fabricate the $TiO_2$ electrode, TTIP (titanium(IV) isopropoxide) was vigorously mixed with ME (2-methoxylethanol) (in the weight ratio of 1:3) to form a metallorganic solution. The metallorganic solution was then spin-coated onto clean conducting fluorine-doped tin oxide (FTO) glasses with a sheet resistivity of 13 Ω/square, followed by annealing at 500 °C for 30 min to form a compact, thin $TiO_2$ layer. A $TiO_2$ paste was applied three times to the top of this compact film using a glass rod to obtain the appropriate thickness. For the first coating (paste 1), the $TiO_2$ colloid mixed with PEG having a molecular weight of 200 000 was used. The second coating, used a $TiO_2$ paste (paste 2) containing a $TiO_2$ colloid and PEG with a molecular weight of 20000. Paste 2 mixed with the light scattering particles of $TiO_2$ (300 nm, 30 wt % in total $TiO_2$) was used for the third (final) coating to reduce light loss by back scattering.

**Device Fabrication of Dye-Sensitized Solar Cells.** The $TiO_2$ film electrode with a $0.4 \times 0.4$ $cm^2$ geometric area was immersed overnight in acetonitrile/tert-butanol mixtures (volume ratio 1:1) containing $2 \times 10^{-4}$ M dye sensitizers. A platinized FTO was used as a counter electrode and contained an active area of 0.16 $cm^2$, produced by adhering a polyester tape with a thickness of 60 $\mu$m. The dye-sensitized photoanode was rinsed with acetonitrile and air-dried. After filling the electrolyte in the spacer, the photoanode was placed on top of the counter electrode, and they were tightly clipped to form a cell. The electrolyte was composed of 0.6 M butylmethylimidazolim (BMII), 0.1 M LiI, 0.5 M 4-*tert*-butylpyridine, 0.03 M $I_2$, 0.5 M guanidinium thiocyanate (GuSCN) dissolved in acetonitrile. The photovoltaic characterizations of the solar cells with a mask ($0.5 \times 0.5$ $cm^2$) were carried out using a 150 W Peccell solar simulator (PEC-L11). Light intensity attenuated by neutral density filter (Optosigma, 078−0360) at the measuring (cell) position, was calibrated to be 100 mW/$cm^2$ according to the reading from a radiant power meter (Oriel, 70260) connected by means of a thermopile probe (Oriel, 70263). Photoelectrochemical characteristic photocurrent density−voltage curves of the DSCs were recorded using a potentiostat/galvanostat (PGSTAT 30, Autolab, Eco-Chemie, The Netherlands).

**Acknowledgment.** This work was financially supported by Academia Sinica, Taiwan. We thank Dr. H.-F. Lu, C.-H. Huang, Dr. Y.-C. Hsu, Dr. Y.-S. Yen, and D.-C. Huang for valuable discussion.

(43) Hsu, Y. C.; Zheng, H.; Lin, J. T.; Ho, K. C. *Sol. Energy Mater. Sol. Cells* **2005**, *87*, 357.